Hydrology Research

Hydrology Research Vol 55 No 3, 301 doi: 10.2166/nh.2024.130

Attribution discernment of climate change and human interventions to runoff decline in Huangshui River Basin, China

Pengquan Wang [a,b,*], Runjie Li[c] and Shengkui Cao[a,d]

[a] School of Geographical Sciences, Qinghai Normal University, Xining 810008, China
[b] School of Civil and Transportation Engineering, Qinghai Minzu University, Xining 810007, China
[c] State Key Laboratory of Plateau Ecology and Agriculture, Qinghai University, Xining 810016, China
[d] Qinghai Province Key Laboratory of Physical Geography and Environmental Process, Xining 810008, China
*Corresponding author. E-mail: wpq1314@126.com; 2016035@qhmu.edu.cn

PW, 0000-0002-2592-3712

ABSTRACT

To achieve sustainable development goals in Huangshui River Basin (HRB), strengthening adaptive water resources management under the dual impact of climate change (CC) and human interventions (HI) is of great significance. Multiple mathematical and statistical methods were employed to determine the runoff trend and breakpoint in HRB. The elasticity of CC and HI on the runoff decline and their contributions were quantitatively discerned based on the Budyko hypothesis, complementary method, and SWAT hydrological model. The results show that (1) the runoff showed a decreasing trend, with a runoff breakpoint in 1990; (2) the elasticity coefficients indicated a 1% increase in P, ET_0, and n, leading to a 2.19% increase, a 1.19% decrease, and a 1.52% decrease in the runoff, respectively; (3) the Budyko framework determined the contribution of CC and HI to runoff decline in HRB to be 37.98–41.86% and 58.14–62.02%, respectively, and that estimated by SWAT hydrological model to be 38.72 and 61.28%, respectively; (4) HI were the primary factor for runoff decline in HRB, where direct anthropogenic disturbances such as water withdrawals and water conservancy project construction were the main drivers. The findings have important scientific significance for water resources planning and management in HRB.

Key words: Budyko hypothesis, climate change, Huangshui River Basin, human interventions, runoff change, SWAT model

HIGHLIGHTS

- We determined the change trend and breakpoint of annual runoff from 1959 to 2014.
- The runoff elasticity was estimated theoretically based on the Budyko hypothesis for 20 mountainous catchments and 5 hydrographic cross-sections in HRB.
- The complementary method calculated the contribution threshold of climate change and human interventions to runoff changes.
- SWAT models were used to discern runoff change attributions.

GRAPHICAL ABSTRACT

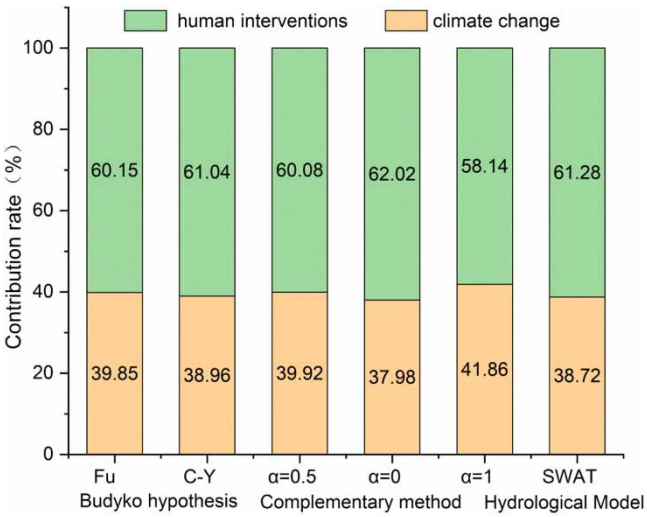

1. INTRODUCTION

Water resources are the key factors limiting socio-economic development, ecological protection, and ecological civilization construction in arid and semi-arid areas. High-intensity human water extraction activities, basin landscape pattern changes, and climate change (CC) have seriously disturbed the intensity, pathways, fluxes, and dynamics of the water cycle. This has resulted in increased uncertainty in the variability of water cycle elements and changes in the spatial and temporal patterns and processes of the terrestrial hydrological situation (Huntington 2006). CC and human interventions (HI) are the two major factors affecting the water cycle (Zhai & Tao 2017). Therefore, identifying the mechanisms of runoff effects due to CC and HI is not only the scientific basis for the adaptive management of water resources under environmental changes but also an intrinsic need for eco-hydrological regulation of sustainable development in watershed systems.

Runoff changes and attribution in watersheds under changing environments have become a research hot topic for Chinese and foreign scholars. This is an important topic emphasized by the Panta Rhei of the International Hydrological Decade (2013–2022) (Montanari *et al.* 2013). Runoff in the northern rivers of China is on a declining trend and suffers from severe droughts and floods, especially in the Yellow River Basin and the Hai River Basin (Feng *et al.* 2016). Whether the main cause of runoff changes is CC or HI, and how to effectively identify and quantitatively separate the impacts of CC and HI on runoff changes, were the main scientific questions of our study. Attribution analysis of runoff changes methods are as follows: (1) statistical regression analysis (Ma *et al.* 2008; Xu 2011; Kong *et al.* 2016); (2) climate elasticity method, total differential method, and complementary method based on the Budyko hypothesis (Xu *et al.* 2014; Zhou *et al.* 2016; Wu *et al.* 2017); (3) hydrological modeling method (Wu *et al.* 2019; Zhou *et al.* 2022). Among them, the Budyko framework is extensively adopted because of its low requirement for historical data, its simple calculation, and the availability of basic physical mechanisms, and the method has been proven to be reasonably credible (Wu *et al.* 2017). The functional analytic formulations of the Budyko hydrothermal coupling framework usually utilize the Choudhury-Yang (C-Y) function (Yang *et al.* 2008) and the Fu function (Fu 1981). The Budyko hypothesis has confirmed good applicability in the Yellow River Basin, Qinghai-Tibet Plateau region, and the Loess Plateau region in China (Sun *et al.* 2007; Yang *et al.* 2015). However, most of the climate elasticity methods can only separate and quantify the contributions of CC and HI to runoff changes at the annual scale, and their application is limited at the smaller spatio-temporal scale. In most studies, the Budyko equation parameters are constant during the baseline period (BP) and perturbation period (PP), and both CC and HI potentially affect equation parameters directly or indirectly (Wang *et al.* 2018). To address the evolution of watershed landscape parameters over time and their discontinuities, the time-varying Budyko framework has been developed and applied (Jiang *et al.* 2015; Xu *et al.* 2021).

The hydrological modeling field has evolved from lumped to distributed models. Lumped models, which treat the watershed as a singular entity, overlook the spatial variability of hydrological phenomena and simplify watershed variables

using average values. These models are typically employed for rainfall–runoff simulations. In contrast, distributed models are characterized by robust physical underpinnings. They not only account for geographic heterogeneity but also elucidate the mechanisms of hydrological processes within a watershed. Consequently, distributed models offer superior capabilities over lumped models in quantifying the impacts of CC and HI on runoff variations across diverse spatial and temporal scales. However, their effectiveness is sometimes constrained by challenges related to model spatio-temporal consistency and inherent uncertainties. Soil & Water Assessment Tool (SWAT) is a process-driven and semi-distributed hydrological model with strong physical mechanisms that was developed by the United States Department of Agriculture (USDA) (Arnold *et al.* 2012). It can better simulate watershed-scale hydrological processes and is widely used for hydrological process simulation and runoff change attribution analysis (Douglas-Mankin *et al.* 2010; Grusson *et al.* 2015; Senbeta & Romanowicz 2021). Furthermore, Water and Energy transfer Processes in Large River basin (WEP-L) (Xu *et al.* 2022), Variable Infiltration Capacity Macro-scale Hydrological mode (VIC) (Yong *et al.* 2013), and Distributed Time Variant Gain Model (DTVGM) (Ning *et al.* 2016) have also been applied to analyze the impacts of CC, subsurface change, and socio-economic water withdrawal on runoff changes. Among the aforementioned hydrological models, the SWAT stands out for its versatility in simulating scenarios pertaining to climate changes and anthropogenic impacts. Notably, SWAT remains the most widely utilized model for investigating runoff responses to climatic variations and human activities, as evidenced by numerous studies (Li *et al.* 2009; Lin *et al.* 2012; Lin *et al.* 2015; Wang *et al.* 2017). Its efficacy in modeling the impact of environmental changes on surface hydrology has been validated across diverse geographical and climatic contexts (Li *et al.* 2022). Consequently, this study employs SWAT to assess the contributions of CC and HI to the runoff alterations in the Huangshui River Basin (HRB).

Given that both the Budyko framework and hydrological models such as SWAT have their respective strengths and limitations, there are uncertainties in the attribution results of runoff changes in the same study area obtained by different scholars (Miao *et al.* 2021). Thus, cross-validation of multiple methods can help us to improve the reliability of hydrological process simulation and runoff change attribution. A single method such as statistical analysis or climate elasticity model has been employed in previous investigations by Chinese researchers (Zhang *et al.* 2014; Du *et al.* 2022) to evaluate the contributions of CC and HI to runoff changes in the HRB, but the comparison with the results of other methods is still lacking and the description of hydro-physical processes is weak. Moreover, the diagnosis of runoff breakpoints is inconsistent and the evaluation results of runoff change attribution are different due to noise interference of runoff time series and the influence of the study time scale. To enhance the credibility of the results, it is necessary to validate the runoff breakpoints using multiple methods and quantify runoff change attribution coupling Budyko framework and SWAT hydrological model.

The HRB, located in eastern Qinghai Province, China, serves as a crucial ecological barrier and is the political, economic, and cultural hub of the province. Confronted with the dual pressures of CC and HI, the basin's rivers predominantly exhibit a declining trend in annual runoff. This trend exacerbates the already critical contradiction between water supply and demand in the HRB, positioning water as the primary limiting factor for sustainable development. Moreover, the implementation of the Lanzhou-Xining Urban Agglomeration Development Planning and Ecological Protection and High-quality Development in the Yellow River Basin amplifies the necessity for integrated water resources management (IWRM). Accurately elucidating the runoff response and its driving forces in the changing environmental context, and discerning the attribution of runoff changes, hold substantial scientific importance. These insights are crucial for adaptive water resources management and the strategic planning of water network projects in the HRB. Therefore, the objectives of our study were as follows: (1) examining runoff change trend and diagnosing runoff breakpoints with multiple methods in HRB; (2) quantifying climate elasticity and human activity elasticity of runoff change in HRB using the Budyko framework; (3) differentiating the impacts of CC and HI on runoff changes using the climate elasticity method, complementary method, and SWAT hydrological model; (4) identifying the major factors and drivers of anthropogenic disturbances affecting runoff changes.

2. RESEARCH MATERIALS AND METHODS

2.1. Study area

Figure 1 shows an overview map of the study area.

The study area is the HRB (100°42′–103°01′E, 36°02′–37°28′N), a major tributary of the upper reaches of the Yellow River, covering a total area of about 16,383 km^2. The HRB originates in Haiyan County of Qinghai Province and is located in the transition zone between the Tibetan and Loess Plateaus, an area of arid and semi-arid continental climate. The average annual precipitation is 300–500 mm, and the average annual temperature is 0.6–7.9 °C. The HRB has a population of

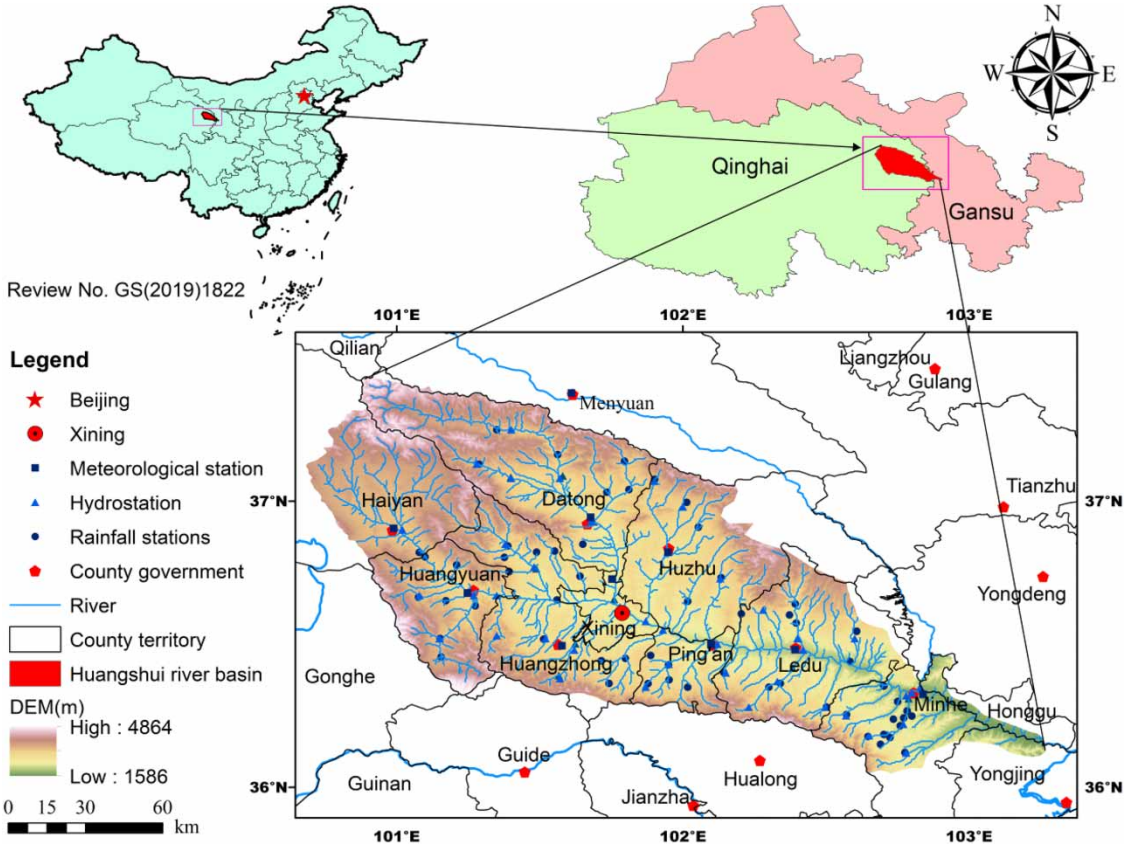

Figure 1 | Overview map of the study area.

about 3.39 million (2018) and constitutes about 60% of the total economy of the province and about 56% of the arable land of the province. HRB's average annual runoff is 2.16 billion m^3. Per capita water resources are about 1/3 of that of the national water resources, and per capita water consumption is 2/3 of that of the national average water resources. The utilization rate is close to 40%, and part of the utilization rate of branch ditch surface water is greater than 50%. The resource and engineering water shortage problems are prominent in HRB. Minhe hydrological station (MHS) is the control station for the HRB.

2.2. Data sources

The digital elevation model (DEM) was derived from a new NASA DEM and an associated product with a 30-m resolution (https://earthdata.nasa.gov/esds). Land use/land cover (LULCs) data were obtained from the Data Center for Resources and Environmental Sciences of the Chinese Academy of Sciences (https://www.resdc.cn). According to the *Classification of Land Use Status (GB/T21010-2017)*, we reclassified LULC data into six aggregate types, including cropland, forestland, grassland, water area, construction land, and unused land. The soil datasets (Xue & Du 2015) were provided by the National Tibetan Plateau/Third Pole Environment Data Center (http://data.tpdc.ac.cn). We calibrated the physicochemical parameters of different soil types for the SWAT model using the Chinese soil database (http://vdb3.soil.csdb.cn/). Spatial data were pre-processed (for instance by projection transformation, reclassification, and clipping) using ArcGIS10.6 software. Figure 2 shows the main data for driving the SWAT model.

The daily precipitation, temperature, relative humidity, wind speed, and sunshine hours were derived from the China National Meteorological Information Center (https://data.cma.cn). Potential evaporation was calculated using the Penman–Monteith equation (Allen *et al.* 1998). Missing meteorological data were acquired by linear interpolation using data from neighboring stations. Batch extraction and processing of daily meteorological data were implemented in Python.

Observed runoff data of the hydrological stations were obtained from the Qinghai Hydrology and Water Resources Forecasting Center. The multi-year average rainfall at representative stations in HRB was derived from the *Qinghai Provincial*

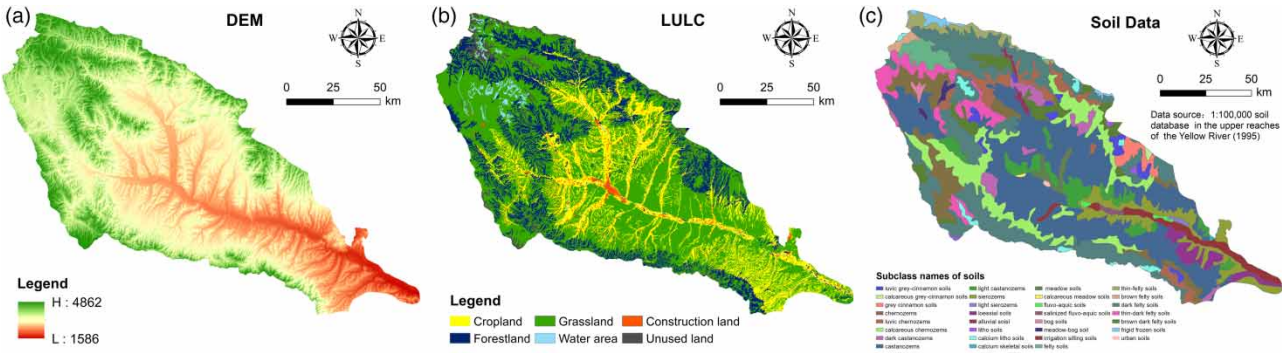

Figure 2 | Data driving the SWAT model.

Hydrology Handbook. The average precipitation and potential evapotranspiration of the HRB were calculated by the Tyson polygon method (Bayraktar *et al.* 2005; Wang *et al.* 2008). The annual NDVI dataset was acquired from the Data Center for Resources and Environmental Sciences of the Chinese Academy of Sciences (https://www.resdc.cn). Vector data such as river system, government residence, and administrative region boundaries were derived from the National Geomatics Center of China (https://www.ngcc.cn/ngcc). Socio-economic data were extracted from *Qinghai Statistical Yearbook* and *Xining National Economic and Social Development Statistical Bulletin*. Water resources development and utilization data were obtained from the *Qinghai Water Resources Bulletin* and *Water Network Planning of the HRB*.

2.3. Methods

Figure 3 exhibits the overall research framework.

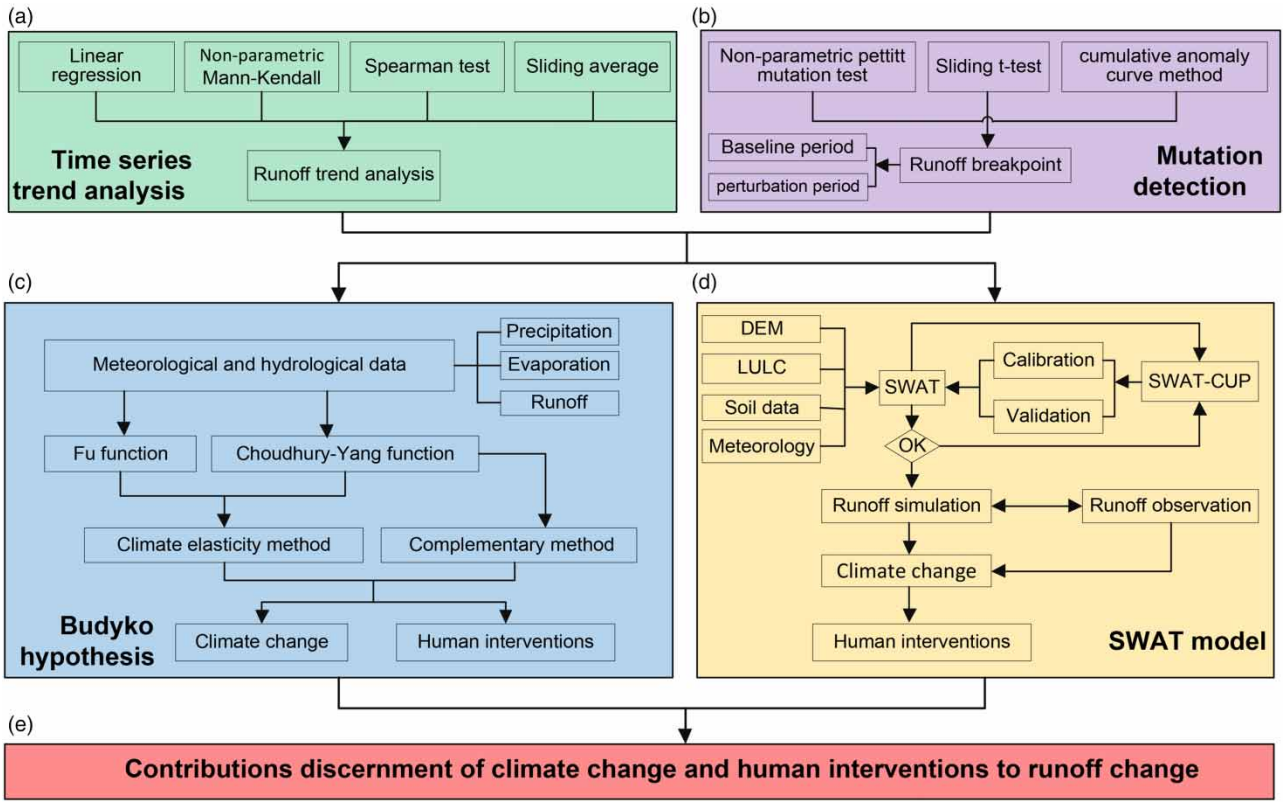

Figure 3 | The overall research framework.

2.3.1. Trend analysis and mutation test

For the analysis of long-term trends in the annual runoff time series spanning from 1959 to 2014, several statistical methods were utilized. These included linear regression, the non-parametric Mann–Kendall test (Woo & Shin 2022), the Spearman test, and the sliding average method (Lou *et al.* 2019). To identify breakpoints in the runoff data, we employed the non-parametric Pettitt mutation test, the sliding *t*-test, and the cumulative anomaly curve method. The entire runoff sequence was segmented into two distinct periods: the BP and the PP, demarcated by the identified abrupt change point.

2.3.2. Attribution analysis of runoff changes based on the Budyko hypothesis

2.3.2.1. Climate elasticity method. The Fu function and C-Y function were employed to discern the contribution of CC and HI to runoff changes, whose analytical equations are as follows (Zhou *et al.* 2015):

$$\frac{E}{P} = 1 + \varphi - (\varphi^{\omega} + 1)^{\frac{1}{\omega}} \quad \omega \in (1, \infty) \quad \text{(Fu function)} \tag{1}$$

$$\frac{E}{P} = \frac{\varphi}{(1 + \varphi^{n})^{\frac{1}{n}}} \quad n \in (0, \infty) \quad (\text{C} - \text{Y function}) \tag{2}$$

where E stands for actual evapotranspiration; P symbolizes precipitation; φ signifies aridity index, $\varphi = \mathrm{ET}_0/P$; ET_0 indicates potential evapotranspiration; ω and n represent the basin landscape parameters, and they are derived using the water balance equation.

The elasticity coefficients of different Budyko equations can all reflect the interaction between climate, vegetation, and runoff. The runoff elasticity coefficient based on the C-Y function is calculated using the following equations:

$$\varepsilon_{\mathrm{P}} = \frac{1 - [\varphi^{n}/(1 + \varphi^{n})]^{1/n+1}}{1 - [\varphi^{n}/(1 + \varphi^{n})]^{1/n}} \tag{3}$$

$$\varepsilon_{\mathrm{ET}_0} = \frac{1}{1 + \varphi^{n}} \cdot \frac{1}{1 - [(1 + \varphi^{n})/\varphi^{n}]^{1/n}} \tag{4}$$

$$\varepsilon_{n} = \frac{\ln\left(\frac{1}{1 + \varphi^{n}}\right) + \varphi^{n} \ln\left(\frac{\varphi^{n}}{1 + \varphi^{n}}\right)}{n(1 + \varphi^{n}) \cdot [(1 + \varphi^{-n})^{1/n} - 1]} \tag{5}$$

If the effect of CC on n is ignored, changes in runoff due to P and ET_0 are attributed to CC, and those due to n are attributed to HI. If the changes in runoff due to P, $\mathrm{ET}_{0,}$ and n are represented by ΔR_{P}, $\Delta R_{\mathrm{ET0,}}$ and ΔR_{n}, respectively, then the amount of change in runoff due to CC is equal to $\Delta R_{\mathrm{P}} + \Delta R_{\mathrm{ET0}}$, and the amount of runoff change due to HI is equal to ΔR_{n}. The attributions of runoff changes are calculated using the climate elasticity method as follows (Xu *et al.* 2014):

$$\Delta R_{\mathrm{P}} = \varepsilon_{\mathrm{P}} \frac{R}{P} \Delta P \tag{6}$$

$$\Delta R_{\mathrm{ET}_0} = \varepsilon_{\mathrm{ET}_0} \frac{R}{\mathrm{ET}_0} \Delta \mathrm{ET}_0 \tag{7}$$

$$\Delta R_{HI} = \Delta R_{n} = \varepsilon_{n} \frac{R}{n} \Delta n \tag{8}$$

where ΔP, Δ_{ET_0}, and Δn represent the change in P, $\mathrm{ET}_{0,}$ and n from BP to the PP, respectively. ε_{P}, $\varepsilon_{\mathrm{ET0}}$, and ε_{n} denote the elasticity coefficients of runoff changes due to P, $\mathrm{ET}_{0,}$ and n, respectively.

2.3.2.2. Complementary method. Zhou *et al.* (2015) demonstrated that for describing the water-energy balance, the C-Y function had a superior analytical form compared to other existing Budyko functions. They proposed a complementary method for the attribution analysis of runoff changes. The complementary method is an efficient method for separating the contributions of CC and HI to runoff changes, where there is no residual between runoff observations and

simulations, and the thresholds of CC and HI on runoff can be estimated when the weighting factors are $\alpha = 0$ and $\alpha = 1$. Especially, $\alpha = 0.5$ was considered to be the best weight for separating and estimating runoff attribution, and the expression of the complementary method was as follows (Zhou *et al.* 2016):

$$\Delta R_{P+\mathrm{ET}_0} = \alpha\left[\left(\frac{\partial R}{\partial P}\right)_1 \Delta P + \left(\frac{\partial R}{\partial \mathrm{ET}_0}\right)_1 \Delta \mathrm{ET}_0\right] + (1-\alpha)\left[\left(\frac{\partial R}{\partial P}\right)_2 \Delta P + \left(\frac{\partial R}{\partial \mathrm{ET}_0}\right)_2 \Delta \mathrm{ET}_0\right] \quad 0 \le \alpha \le 1 \tag{9}$$

$$\Delta R_{\mathrm{n}} = \alpha\left[P_2 \Delta\left(\frac{\partial R}{\partial P}\right) + ET_{0,2}\Delta\left(\frac{\partial R}{\partial \mathrm{ET}_0}\right)\right] + (1-\alpha)\left[P_1 \Delta\left(\frac{\partial R}{\partial P}\right) + \mathrm{ET}_{0,1}\Delta\left(\frac{\partial R}{\partial \mathrm{ET}_0}\right)\right] \quad 0 \le \alpha \le 1 \tag{10}$$

2.3.3. Attribution analysis of runoff changes based on the SWAT hydrological model

SWAT is a multi-process model that integrates hydrology, ecology, agriculture, and water quality. We utilized the SWAT model to discretize the HRB into 85 sub-basins (SUBs) and 1,480 hydrological response units (HRUs). A preheat period of 3 years was set to simulate the monthly runoff of the study area from 1962 to 2014. The potential evapotranspiration (expressed with ET_0) was calculated through the FAO-56 Penman–Monteith equation in the SWAT model. Surface runoff was computed using Soil Conservation Service Curve Number (SCS-CN) and the intra-channel confluence process was calculated using the Muskingum principle. Twenty-eight parameters were selected to calibrate and validate the SWAT model using the Sequential Uncertainty Fitting Ver-2 (SUFI-2) algorithm, which was built and introduced into the SWAT-CUP software. The model was set up for an initial run of 500 times. The larger the *t*-Stat determined by the SUFI-2 algorithm, the more sensitive the parameter is. Besides, the smaller the *p*-value, the more important the parameter is. We used the parameters with $p < 0.1$ as key sensitive parameters and tuned the parameters using a combination of automatic and manual calibration until the Nash–Sutcliffe efficiency (NSE) no longer could be improved (Abbaspour *et al.* 2015). We assessed the SWAT model performance by using four indicators (Abou Rafee *et al.* 2019), including determination coefficient (R^2), Nash–Sutcliffe efficiency (NSE), percentage bias (PBIAS), and root mean square error (RMSE) to observations of standard deviation ratio (RSR) (Ren *et al.* 2021).

Simulation, calibration, and validation of runoff in the SWAT model are better suited to the runoff stabilization period (Kannan *et al.* 2007). Therefore, the study period was divided into a BP (1959–1990) and a PP (1991–2014). The runoff changes were considered to be caused by both CC and HI, and the total runoff changes were computed from the difference between the average observed runoff in the BP and the PP (Senbeta & Romanowicz 2021). Thus, the total runoff changes ($\Delta Q_{\mathrm{total}}$) were defined as follows:

$$\Delta Q_{\mathrm{total}} = \Delta Q_{\mathrm{CC}} + \Delta Q_{\mathrm{HI}} = Q_{\mathrm{obs}}^{\mathrm{PP}} - Q_{\mathrm{obs}}^{\mathrm{BP}} \tag{11}$$

The climatic factors in the SWAT runoff simulation underwent dynamic changes from the BP to the PP, while the LULC remained constant. Hence, the amount of runoff change contributed by CC was considered as the difference between simulated mean runoff in the PP and BP.

$$\Delta Q_{\mathrm{CC}} = Q_{\mathrm{sim}}^{\mathrm{PP}} - Q_{\mathrm{sim}}^{\mathrm{BP}} \tag{12}$$

Thus, the contribution of HI to the change in runoff was calculated as the difference between $\Delta Q_{\mathrm{total}}$ and ΔQ_{CC} as follows:

$$\Delta Q_{\mathrm{HI}} = (Q_{\mathrm{obs}}^{\mathrm{PP}} - Q_{\mathrm{obs}}^{\mathrm{BP}}) - (Q_{\mathrm{sim}}^{\mathrm{PP}} - Q_{\mathrm{sim}}^{\mathrm{BP}}) \tag{13}$$

The rates of change in runoff due to CC and HI were expressed as follows:

$$\begin{aligned} \eta_{\mathrm{CC}} &= \frac{\Delta Q_{\mathrm{CC}}}{\Delta Q_{\mathrm{total}}} \times 100\% \\ \eta_{\mathrm{HI}} &= \frac{\Delta Q_{\mathrm{HI}}}{\Delta Q_{\mathrm{total}}} \times 100\% \end{aligned} \tag{14}$$

where $\Delta Q_{\mathrm{total}}$ stands for the change in runoff from the BP to the PP; ΔQ_{CC} represents the amount of change in runoff due to CC; ΔQ_{HI} signifies the amount of change in runoff caused by HI; $Q_{\mathrm{obs}}^{\mathrm{PP}}$ and $Q_{\mathrm{sim}}^{\mathrm{PP}}$ denotes average observed runoff and average

simulated runoff in the PP, respectively; Q_{obs}^{BP} and Q_{sim}^{BP} symbolize average observed runoff and average simulated runoff in the BP, respectively ; η_{CC} indicates the contribution rate of runoff changes due to CC ; η_{HI} shows the contribution rate of runoff changes caused by HI.

3. RESULTS

3.1. Runoff trends and breakpoints

The runoff trend of MHS in HRB is displayed in Figure 4(a), and the results of the runoff breakpoints test are exhibited in Figure 4(b)–4(d), respectively. The comprehensive results for runoff trends and breakpoints are presented in Table 1. Linear trend analysis of the runoff time series showed that the tendency slope was −0.212, indicating a decreasing trend in the runoff on the 1959–2014 time scale ($p < 0.05$). However, the results of the Spearman and Mann–Kendall tests indicated that the trend of runoff variation was not significant. The Pettitt test revealed that possible breakpoints were 1990 and 1994 ($p < 0.5$); the sliding t-test demonstrated that the possible breakpoints were 1980, 1990, 1994, and 2004 ($p < 0.05$); and the cumulative anomaly method suggested that the possible breakpoints were 1968, 1982, and 1990 ($p < 0.05$). According to the three mutation detection results, the study confirmed that the runoff breakpoint of MHS in the HRB was in 1990.

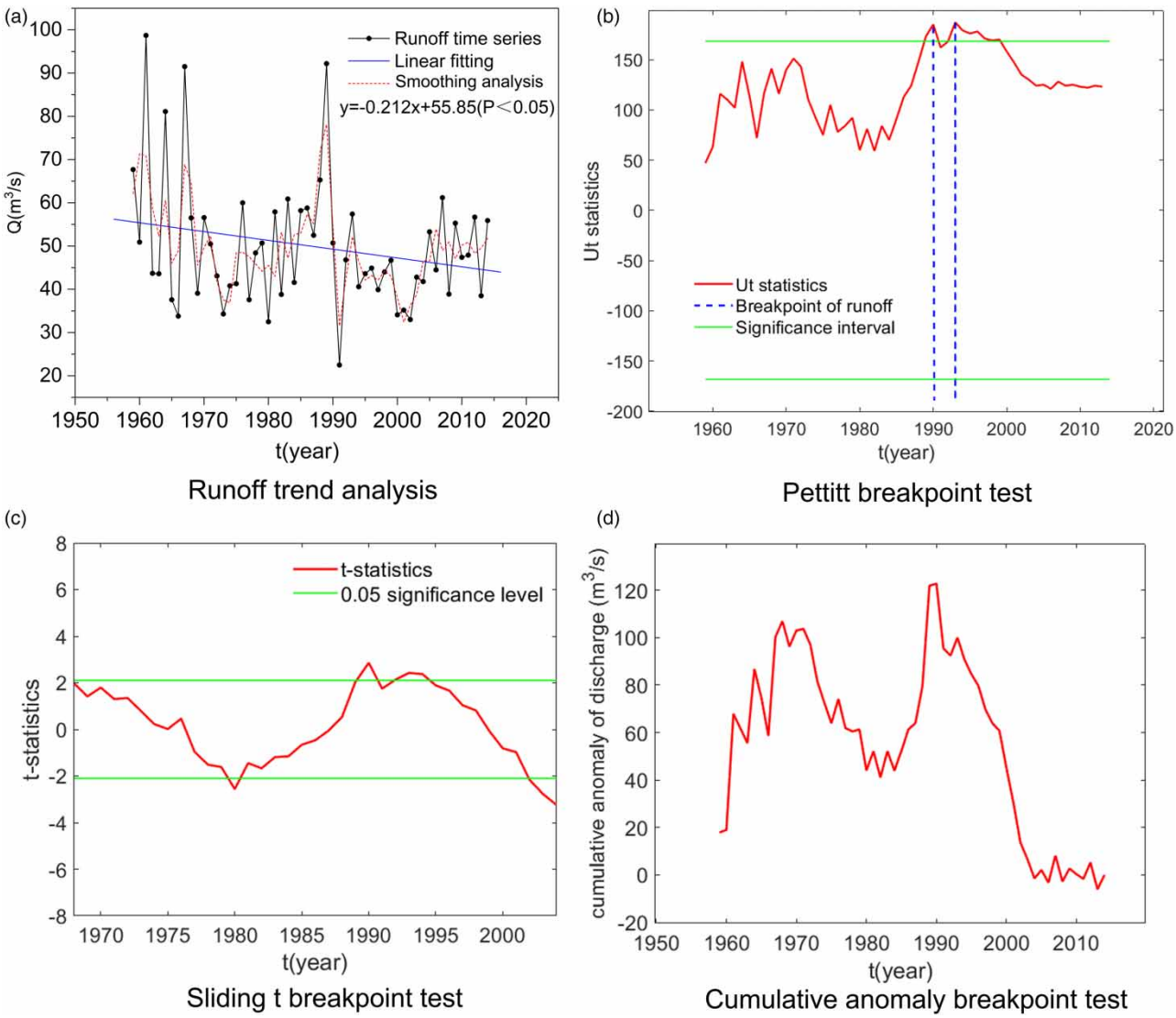

Figure 4 | Runoff trends and mutation detection.

Table 1 | Integrated results of runoff trend and breakpoints detection

		Trend			Breakpoint		
HRB	**Time series**	**Linear regression****	**Spearman**	**M-K**	**Pettitt test***	**Sliding *t*-test****	**Cumulative anomaly****
MHS	1959–2014	−0.212	ns	ns	1990, 1993	1980, 1990, 1994, 2004	1968, 1980, 1990

Note: '*' indicates $p < 0.5$; '**' indicates $p < 0.05$; 'ns' indicates not significant.

3.2. Attribution of runoff changes based on the Budyko hypothesis

Based on the results of runoff breakpoints detection and collected rainfall and evapotranspiration time series data, we delineated the study time domain into a BP (1959–1990) and a PP (1990–2014). Using the multi-year average precipitation, runoff, and potential evapotranspiration data for the 20 mountainous catchments and 5 hydrographic cross-sections in the study area, Figure 5(a) displays the Budyko curves and sample point data based on the C-Y function. The relationship between climate elasticity of runoff changes and aridity index (expressed with $\varphi = \mathrm{ET}_0/P$) is shown in Figure 5(b) and 5(c), and the elasticity of runoff with change in watershed landscape parameter (denoted by n) under different aridity indices is exhibited in Figure 5(d). The watershed landscape parameter (n) was mainly distributed between 1.0 and 2.0, and the aridity index (φ)

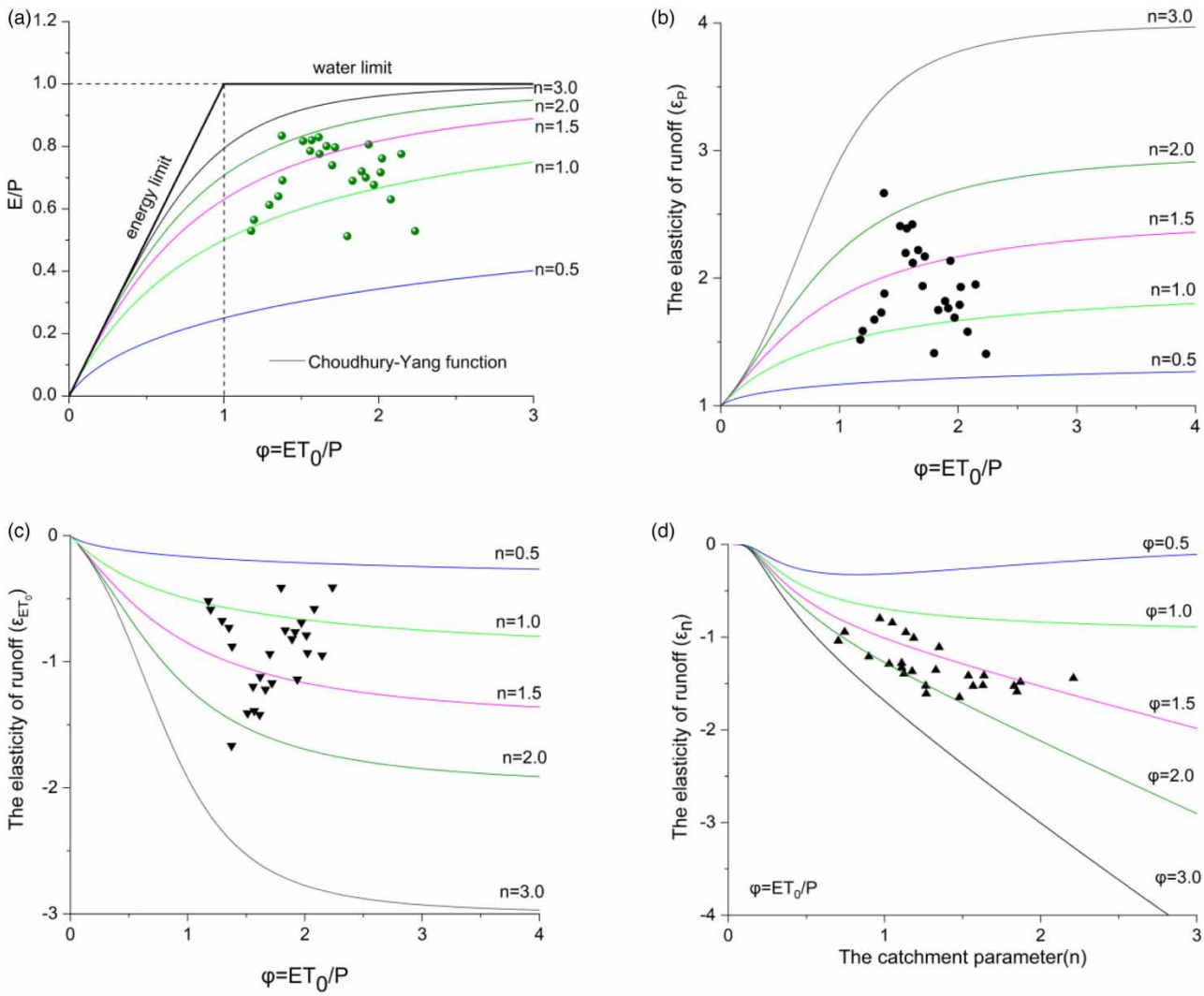

Figure 5 | Relationship between elasticity of the runoff and aridity index/landscape parameter.

was mostly distributed between 1.5 and 2.0. The runoff elasticity was related to climatic conditions (expressed by aridity index) and watershed landscape parameter (expressed by n), and the absolute value of runoff elasticity increased with the increase of aridity index φ and parameter n. The runoff elasticity for potential evapotranspiration (ET_0) and watershed landscape parameter (n) were both negative and the runoff elasticity for precipitation (P) was positive. This means that an increase in ET_0 and n will lead to a decrease in the runoff, and an increase in P will result in an increase in the runoff.

The results of the analysis of runoff elasticity changes of MHS in HRB are presented in Table 2. The potential evapotranspiration (ET_0) and aridity index (φ) increased by 1.93 and 4.24%, respectively, and the precipitation (P) and runoff (R) decreased by 2.27 and 16.67%, respectively, during the PP in comparison to the BP. The watershed landscape parameters (n) calculated by the Fu and C-Y functions all showed an increase in PP compared with BP, indicating that the influence of human activities tended to be enhanced. Based on the multi-year average hydro-meteorological data from 1959 to 2014, the elasticity coefficients calculated using the C-Y equation were 2.19 for P, −1.19 for ET_0, and −1.52 for n. The elasticity coefficients demonstrated that a 1% increase in P, ET_0, and n gave rise to a 2.19% increase, a 1.19% decrease, and a 1.52% decrease in the runoff, respectively. Obviously, the sensitivity of runoff to P was higher than ET_0 and basin landscape changes in HRB.

Table 3 presents the results of the attribution analysis of runoff changes under the Budyko framework. The calculations using the Fu equation suggested that the contribution of CC to runoff reduction was 39.85% (P contributed 27.51% and ET_0 contributed 12.34%) and the contribution of HI to runoff attenuation was 60.15%. Using the C-Y equation, it was found that the contribution of CC to the decrease of runoff was 38.96% (P contributed 27.04% and ET_0 contributed 11.92%) and the contribution of HI to the reduction of runoff was 61.04%. The complementary method usually used $\alpha = 0.5$ as the best estimate for the weighting factor, which calculated the contribution of CC to runoff decrease to be 39.92% (P contributed 27.47% and ET_0 contributed 12.45%) and the contribution of HI to runoff reduction was 60.08%.

Table 2 | Analysis of hydro-meteorological factors and runoff elasticity changes of MHS in HRB

Parameters		Baseline period 1959–1990	Perturbation period 1991–2014	Simulation period 1959–2014	Change amount
Hydrothermal parameters	P/mm	511.9	500.3	504.5	−11.6
	ET_0/mm	846.1	862.4	854.2	16.2
	R/mm	110.4	92.0	102.5	−18.4
	$\varphi = ET_0/P$	1.65	1.72	1.69	0.07
Fu function	ω	2.27	2.38	2.30	0.12
	ε_p	2.10	2.23	2.14	0.12
	ε_{ET_0}	−1.10	−1.23	−1.14	−0.12
	ε_ω	−2.12	−2.26	−2.19	−0.15
C-Y function	n	1.55	1.67	1.59	0.12
	ε_p	2.14	2.28	2.19	0.13
	ε_{ET_0}	−1.14	−1.28	−1.19	−0.13
	ε_n	−1.46	−1.60	−1.52	−0.14

Table 3 | Results of attribution analysis of runoff changes using the Budyko framework

Budyko function and method		Runoff changes (mm)				Contribution rate of runoff change (%)			
		ΔR_p	ΔR_{ET_0}	ΔR_n	ΔR_{total}	η_p	η_{ET_0}	η_{CC}	η_{HI}
Fu function		−5.15	−2.31	−11.27	−18.73	27.51	12.34	39.85	60.15
C-Y function		−5.05	−2.23	−11.40	−18.67	27.04	11.92	38.96	61.04
Complementary method	$\alpha = 0.5$	−5.10	−2.31	−11.16	−18.58	27.47	12.45	39.92	60.08
	$\alpha = 0$	−4.85	−2.21	−11.52	−18.58	26.10	11.89	37.98	62.02
	$\alpha = 1$	−5.36	−2.42	−10.80	−18.58	28.84	13.02	41.86	58.14

Note: The watershed parameter (n) was estimated using the C-Y equation in the complementary method.

The estimates of runoff changes attributed to the above three methods were similar, and HI played a primary role in runoff changes. The complementary method can determine the upper and lower limits of CC and HI impacts on runoff using weighting factors $\alpha = 0$ and $\alpha = 1$. The thresholds for CC contribution to runoff reduction were 37.98–41.86% and for HI contribution to runoff decrease were 58.14–62.02%. The attribution results of runoff changes identified by the Fu equation and C-Y equation were within the thresholds estimated by the complementary method. The runoff reductions calculated by the Fu equation, C-Y equation, and complementary method were 18.73, 18.67, and 18.58 mm, respectively, and the observed runoff reduction was 18.4 mm. The relative errors between the estimated and measured values were 1.79, 1.45, and 0.98%, respectively, reflecting that the calculation accuracy of the Budyko hypothesis was high. Hence, the results of the attribution of runoff changes based on the Budyko framework were reliable.

3.3. Attribution of runoff changes based on the SWAT hydrological model

By setting a warm-up period of 3 years (1959–1961), a calibration period (1962–1980), and a validation period (1981–1990), we calibrated the SWAT model based on the monthly observed runoff at MHS of the HRB from 1962 to 1990. The more sensitive 10 parameters were selected from 28 parameters and their fitted values were achieved by parameter calibration and manual adjustment (Table 4). Figure 6 shows simulated versus observed flow processes for the calibration and validation periods and their simulated performance of the SWAT model. R^2, NSE, RSR, and PBIAS for the calibration period were 0.76, 0.71, 0.54, and −7.64%, respectively; R^2, NSE, RSR, and PBIAS for the validation period were 0.78, 0.74, 0.51, and 11.7%, respectively. Based on the evaluation indices and evaluation grade of SWAT simulation results (Abou Rafee *et al.* 2019), the model performance achieved a 'good' level. The average value of simulated flow in 1962–1990 was 51.64 m^3/s, and that of measured flow was 53.48 m^3/s, with a relative error of only 3.44%. Thus, the overall performance of the SWAT model was good and could be employed for HRB runoff simulation.

The attribution results of runoff changes calculated by the SWAT model in HRB are presented in Table 5. The contribution of CC to runoff changes was 38.72% and that of HI was 61.28%. Hence, the impact of HI on runoff changes was more obvious than that of CC.

4. DISCUSSION

4.1. Analysis of variability in attribution results of runoff changes

We determined the impact of CC and HI on runoff using the runoff elasticity method based on the Budyko hypothesis, complementary method, and SWAT hydrological model, respectively. The Budyko hypothesis determined the contribution of CC to runoff changes to be 37.98–41.86% and that of HI to be 58.14–62.02%. And SWAT hydrological model estimated the contribution of CC and HI to runoff changes to be 38.72 and 61.28%, respectively. Although the Budyko framework and SWAT model were substantially different in terms of computational principles and time scales, attribution results of runoff changes were close. Zhang *et al.* (2014) utilized the change rate of the accumulation slope method to determine the contribution of CC

Table 4 | Key sensitive parameters and their optimal values

Sensitivity sorting	Parameter name	Parameter description	Range	Best parameter	|t|	p
1	R_CN2.mgt	SCS runoff curve number	−0.5 ~ 0.5	−0.021	16.04	<0.01
2	R_SOL_BD().sol	Moist bulk density ($g \cdot cm^{-3}$)	−0.5 ~ 0.5	0.201	6.82	<0.01
3	V_CANMX.hru	Maximum canopy storage (mm)	0 ~ 100	20.001	6.16	<0.01
4	R_SOL_K().sol	Saturated hydraulic conductivity ($mm \cdot h^{-1}$)	−0.5 ~ 0.5	−0.386	4.61	<0.01
5	V_ALPHA_BNK.rte	Base flow alpha factor for bank storage	0 ~ 1	0.329	3.67	<0.01
6	V_HRU_SLP.hru	Average slope ($m \cdot m^{-1}$)	0 ~ 1	0.191	3.45	<0.01
7	R_SOL_Z().sol	Depth from soil surface to bottom (mm)	−0.5 ~ 0.5	−0.249	2.69	<0.01
8	V_ESCO.hru	Soil evaporation compensation factor	0 ~ 1	0.989	2.02	0.04
9	R_TLAPS.sub	Temperature lapse rate ($°C \cdot km^{-1}$)	−0.5 ~ 0.5	−0.209	1.74	0.08
10	V_SMTMP.bsn	Snowmelt base temperature (°C)	−5 ~ 5	−4.91	1.69	0.09

Note: Parameters beginning with 'V_' and 'R_' indicate a replacement and a relative change to the initial parameter values, respectively.

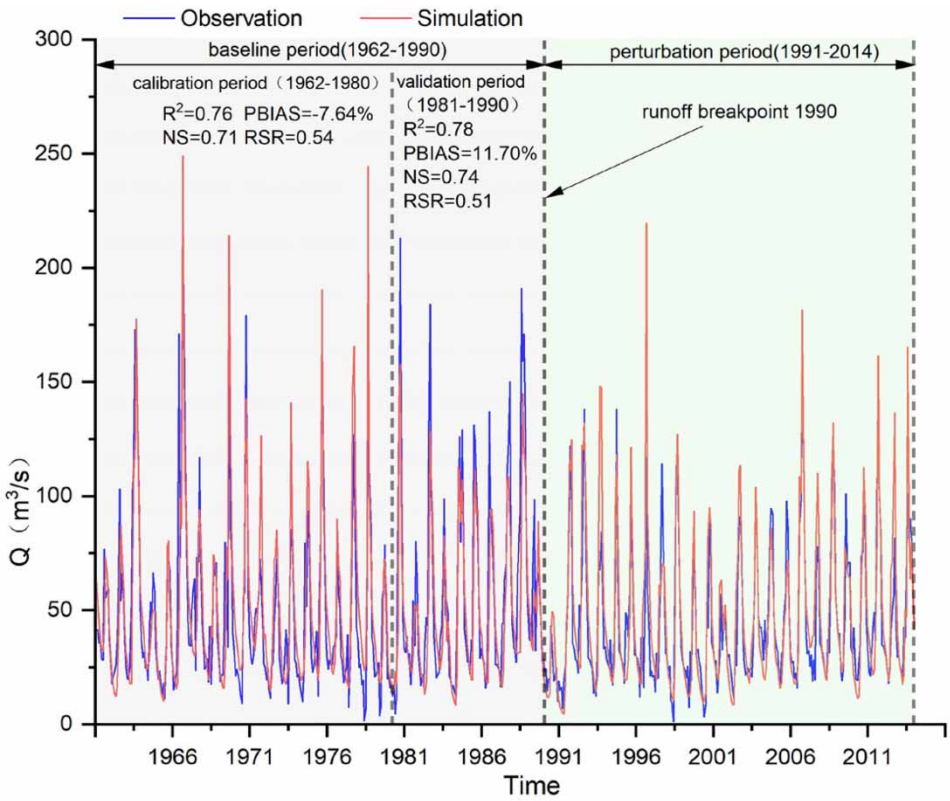

Figure 6 | Simulated and observed flow processes and simulation performance.

Table 5 | Runoff changes and attribution discernment based on SWAT simulation in HRB

Average flow (m^3/s)				Flow changes (m^3/s)			Contribution rate (%)	
Q_{obs}^{BP}	Q_{sim}^{BP}	Q_{obs}^{PP}	Q_{sim}^{PP}	ΔQ_{total}	ΔQ_{CC}	ΔQ_{HI}	η_{CC}	η_{HI}
53.48	51.64	44.13	48.02	−9.35	−3.62	−5.73	38.72	61.28

to runoff reduction in the 1966–2010 periods and found that it was 35.46% in HRB, and that of HI was 64.54%. Du *et al.* (2022) investigated the attribution of runoff changes on different time scales based on the Fu function and concluded that landscape had the most significant impact on runoff, followed by precipitation, and potential evapotranspiration had the least impact. The results of existing studies were generally consistent with our conclusion that human activities were the primary factor that contributed to the decrease in the runoff. It was worth noting that the watershed landscape parameter (n) in the Budyko framework was influenced by both CC and HI, and that CC could indirectly affect runoff changes by influencing the watershed landscape, which may result in a small contribution of CC to runoff changes under the Budyko framework (Miao *et al.* 2021).

4.2. Analysis of anthropogenic drivers of runoff reduction

4.2.1. Impact of economic and social development on the runoff

Xining City, as the focal point of economic and social development within the HRB, is also a significant area in terms of water consumption. Therefore, we selected Xining as a representative area to investigate the impact of economic and social development on runoff dynamics. Figure 7(a) and 7(b) depict the evolution of gross domestic product (GDP) and population of the Xining area in the middle reaches of the HRB since 1949. Large-scale population growth and GDP development increased

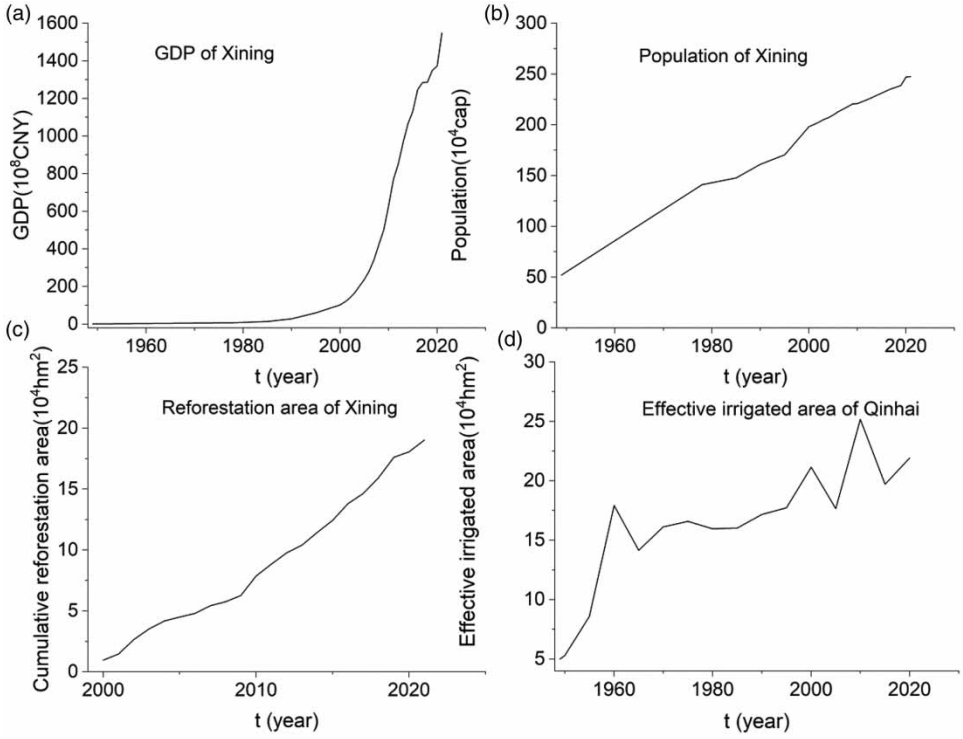

Figure 7 | Changes in economic and social development indicators.

the consumption of water resources, which led to reduced runoff. Since 2000, Qinghai provincial government implemented 'returning farmland to the forest', which caused the local ecological environment to greatly improve. The cumulative area of returning farmland to forestland (also grassland) in the Xining area from 2000 to 2020 was about 0.19 million hm^2 (Figure 7(c)). The ecological restoration project enhanced the soil and water conservation capacity of the watershed but reduced the capacity of surface flow production. Existing studies have demonstrated that runoff coefficients decrease with increasing vegetation cover and that even the hydrologic impact of vegetation in reducing surface runoff exceeds that of CC (Fan *et al.* 2015; Gu *et al.* 2018). Figure 7(d) exhibits the change in the effective irrigated area in Qinghai Province since 1949. The arable land area in HRB accounts for about 56% of that in the Qinghai Province. From 1950 to 1990, the effective irrigated area in Qinghai Province increased by 2.24 times, and from 1990 to 2010, it increased by 46.7%. The substantial increase in irrigated farmland area inevitably triggered an increase in irrigation water withdrawal, which exacerbated the depletion of water resources in HRB.

4.2.2. Impact of water resources development and utilization on the runoff

According to runoff data of MHS from 1959 to 2014 (Figure 8(a)) and *Qinghai Provincial Hydrology Handbook*, the multi-year average natural runoff of MHS is 2.080 billion m^3, and the multi-year average observed runoff is 1.572 billion m^3, which is 24.4% less than the natural flow. In particular, the annual average observed runoff at the MHS had decreased by 31.0% since 1990 compared to the natural runoff, which further confirmed that choosing 1990 as the runoff breakpoint was acceptable. Figure 8(b) shows the cumulative reservoir capacity curve (including flood ponds and silt dams) from the 1950s to the present in HRB. The cumulative reservoir capacity was only 730,000 m^3 at the end of the 1950s, reached 176.59 million m^3 at the end of the 1990s, and reached 407.86 million m^3 at the end of the 2010s. The reservoir storage and its water supply to industry and agriculture led to the destruction of the hydrological consistency conditions, which reduced the surface runoff of downstream rivers. We also investigated the development and utilization rate of water resources of 22 typical branch ditches in HRB (Figure 8(c)), among which there were 7 branch ditches with surface water resources development and utilization rate of over 40%. The increase in water resources development and utilization degree was bound to cause runoff reduction.

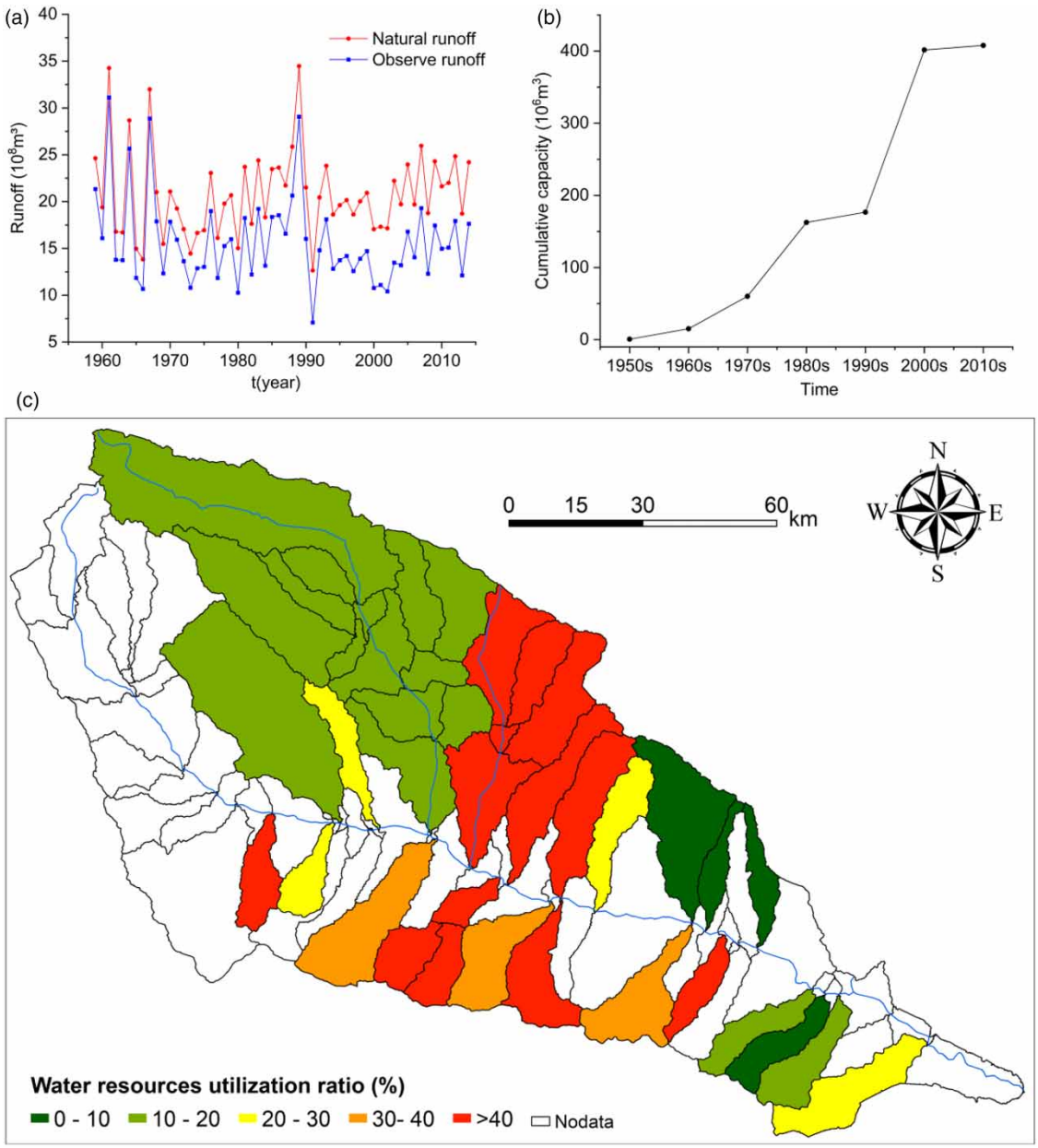

Figure 8 | Water resources development and utilization data in HRB.

4.2.3. Impact of land use change on the runoff

The reclassified land use/land covers (LULCs) of the late 1980s and 2010 were utilized to generate a land use transfer Sankey map between the BP and PP (Figure 9(a)). The primary land use types in the study area were grassland and cropland, with grassland which was largely converted to cropland, cropland which was chiefly converted to construction land and forestland, and a smaller amount of building land and unused land which was converted to other land types. There was very little conversion of construction land and unused land to other land types. From the 1980s to 2010, the area of cropland and grassland showed a decreasing trend, and the area of forestland, water area, and construction land displayed an increasing trend, with a 16.1% increase in construction land and a 12.2% increase in water area. The increase in water area was predominantly caused by the construction of a large number of reservoirs. Reservoir storage will inevitably diminish the river discharge flow during the abundant water period and will increase the ineffective evaporation from the water surface,

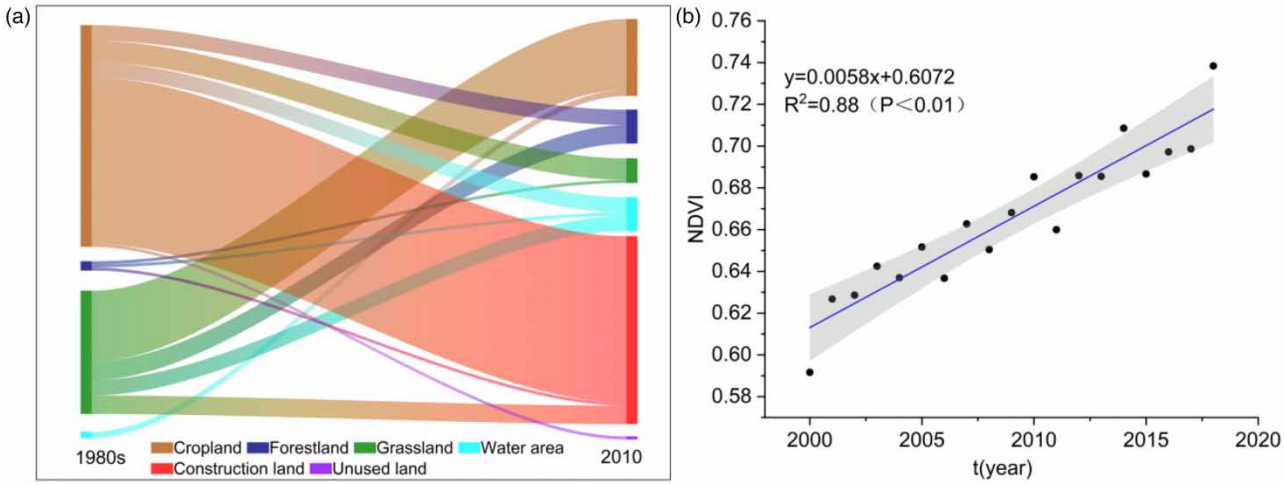

Figure 9 | Land transfer and vegetation index.

thus leading to a decrease in the runoff. Although the increase in construction land will increase surface flow production efficiency, the hydrological effect is much less significant than direct human activities such as water extraction and dam construction. Figure 9(b) shows that Normalized Difference Vegetation Index (NDVI) in the study area was increasing from 2000 to 2018 ($p < 0.01$), and the implementation of 'returning farmland to forestland' considerably increased the surface vegetation cover. Meanwhile, 'green water' accounts for an increasing proportion of the flux in the water cycle. Green water flow and green water storage will lead to the reduction of surface runoff (Liu *et al.* 2023).

4.3. Uncertainty analysis

The effects of CC and HI on runoff are different at different spatial and temporal scales, the interactions between the two are complex, and it is difficult to separate them completely. Uncertainty in the results of the attribution of runoff changes in this study arose principally from the following aspects. (1) The division of the BP and PP was determined by the detection accuracy of runoff time series breakpoint, and the spatio-temporal harmony and spatio-temporal scale effects of the hydrological model had significant effects on the results. (2) The physical meaning and mathematical expression of the parameter $n(\omega)$ in the Budyko equation is still unclear, and the parameters affected by the water conservancy project and watershed landscape pattern dynamic time-varying are not sufficiently represented. (3) The role of CC and HI is interactive, and the two factors are not completely independent. (4) Geographic divergence and temporal variability of hydro-meteorological parameters and watershed landscape patterns in the SWAT hydrological model give rise to differences in eco-hydrological processes at different spatial and temporal scales. The primary sources of uncertainty in the SWAT model are associated with input data, model parameters, and the structure of calibration tools. These factors collectively contribute to unavoidable deviations in model simulations. More importantly, the uncertainty in contribution to runoff changes due to the 'equifinality for different parameters' of the hydrological model cannot be ignored.

5. CONCLUSION

We used the Budyko hypothesis and SWAT hydrological model to quantitatively differentiate the attribution of CC and HI to runoff changes, which is important for adaptive water resources management in HRB. The main findings of the study are as follows:

(1) The runoff in HRB on the time scale of 1959–2014 showed a decreasing trend, and the average decrease rate of runoff was 0.212 $m^3/s{\cdot}a^{-1}$ (0.44 mm/a). The significant runoff breakpoint was 1990, and the study period was divided into BP (1959–1990) and PP (1991–2014). The average runoff in PP had decreased by 18.4 mm compared with the BP.
(2) The Budyko framework determined the contribution of CC to runoff changes in HRB to be 37.98–41.86% and that of HI to be 58.14–62.02%. The SWAT hydrological model estimated the contribution of CC and HI to runoff decline to be 38.72 and 61.28%, respectively. The study concluded that HI was the primary factor in runoff decline, and direct human

activities such as economic and social water withdrawals and water conservancy project construction had a substantial impact on runoff changes.

(3) The main reasons for runoff decline driven by HI were: (a) the increase in water consumption for domestic, industrial, and agricultural use to support economic and social development; (b) increased watershed storage and disruption of natural runoff processes owing to reservoir construction; (c) increase in green water flux and green water storage because of reforestation. However, how to effectively and quantitatively distinguish the effects of different anthropogenic disturbances (e.g., Land use/cover change (LUCC), dam operation, and water extraction) on hydrological processes requires further investigation and research.

ACKNOWLEDGEMENTS

The authors would like to thank the reviewers and editors for their insightful comments on improving the paper. Besides, the authors would like to express their gratitude to EditSprings (https://www.editsprings.cn) for the expert linguistic services provided. This work was supported by the Qinghai Minzu University Planning Project [grant number: 23GH14] and the Applied Basic Research Project of Qinghai Province in China [grant number: 2024-ZJ-773].

DATA AVAILABILITY STATEMENT

Data cannot be made publicly available; readers should contact the corresponding author for details.

CONFLICT OF INTEREST

The authors declare there is no conflict.

REFERENCES

Abbaspour, K. C., Rouholahnejad, E., Vaghefi, S., Srinivasan, R., Yang, H. & Kløve, B. 2015 A continental-scale hydrology and water quality model for Europe: Calibration and uncertainty of a high-resolution large-scale SWAT model. *Journal of Hydrology* **524**, 733–752. doi:10.1016/j.jhydrol.2015.03.027.

Abou Rafee, S. A., Uvo, C. B., Martins, J. A., Domingues, L. M., Rudke, A. P., Fujita, T. & Freitas, E. D. 2019 Large-scale hydrological modelling of the Upper Paraná River Basin. *Water* **11**, 5. doi:10.3390/w11050882.

Allen, R. G., Pereira, L. S., Raes, D. & Smith, M. 1998 *Crop Evapotranspiration: Guidelines for Computing Crop Water Requirements*. Irrigation and Drainage Paper No 56. Food and Agriculture Organization of the United Nations (FAO), Rome, Italy.

Arnold, J. G., Moriasi, D. N., Gassman, P. W., Abbaspour, K. C., White, M. J., Srinivasan, R., Santhi, C., Harmel, R. D., Griensven, A. V., Liew, M., Kannan, N. & Jha, M. K. 2012 SWAT: Model use, calibration, and validation. *Transactions of the ASABE* **55** (4), 1491–1508. doi:10.13031/2013.42256.

Bayraktar, H., Turalioğlu, F. S. & Şen, Z. 2005 The estimation of average areal rainfall by percentage weighting polygon method in Southeastern Anatolia Region, Turkey. *Atmospheric Research* **73**, 149–160. doi:10.1016/j.atmosres.2004.08.003.

Douglas-Mankin, K. R., Srinivasan, R. & Arnold, J. G. 2010 Soil and Water Assessment Tool (SWAT) model: Current developments and applications. *Transactions of the ASABE* **53** (5), 1423–1431. doi:10.13031/2013.34915.

Du, J., Cai, Y., Liu, X., Wang, G. & Min, M. 2022 Attribution analysis of runoff in the Huangshui River based on the Budyko hypothesis. *China Rural Water and Hydropower* (07), 116–121.

Fan, X., Ma, Z., Yang, Q., Han, Y. & Mahmood, R. 2015 Land use/land cover changes and regional climate over the Loess Plateau during 2001–2009. Part II: Interrelationship from observations. *Climatic Change* **129** (3–4), 441–455. doi:10.1007/s10584-014-1068-5.

Feng, X., Cheng, W., Fu, B. & Lü, Y. 2016 The role of climatic and anthropogenic stresses on long-term runoff reduction from the Loess Plateau, China. *The Science of the Total Environment* **571**, 688–698. doi:10.1016/j.scitotenv.2016.07.038.

Fu, B. 1981 On the calculation of the evaporation from land surface. *Scientia Atmospherica Sinica* **5** (01), 23–31.

Grusson, Y., Sun, X., Gascoin, S., Sauvage, S., Raghavan, S., Anctil, F. & Sáchez-Pérez, J.-M. 2015 Assessing the capability of the SWAT model to simulate snow, snow melt and streamflow dynamics over an alpine watershed. *Journal of Hydrology* **531**, 574–588. doi:10.1016/J.JHYDROL.2015.10.070.

Gu, C., Mu, X., Gao, P., Zhao, G. & Sun, W. 2018 Changes in run-off and sediment load in the three parts of the Yellow River basin, in response to climate change and human activities. *Hydrological Processes* **33** (4), 585–601. doi:10.1002/hyp.13345.

Huntington, T. G. 2006 Evidence for intensification of the global water cycle: Review and synthesis. *Journal of Hydrology* **319** (1–4), 83–95. doi:10.1016/J.JHYDROL.2005.07.003.

Jiang, C., Xiong, L., Wang, D., Liu, P., Guo, S. & Xu, C.-y. 2015 Separating the impacts of climate change and human activities on runoff using the Budyko-type equations with time-varying parameters. *Journal of Hydrology* **522**, 326–338. doi:10.1016/J.JHYDROL.2014.12.060.

Kannan, N., White, S. M., Worrall, F. & Whelan, M. J. 2007 Sensitivity analysis and identification of the best evapotranspiration and runoff options for hydrological modelling in SWAT-2000. *Journal of Hydrology* **332** (3–4), 456–466. doi:10.1016/J.JHYDROL.2006.08.001.

Kong, D., Miao, C., Wu, J. & Duan, Q. 2016 Impact assessment of climate change and human activities on net runoff in the Yellow River Basin from 1951 to 2012. *Ecological Engineering* **91**, 566–573. doi:10.1016/J.ECOLENG.2016.02.023.

Li, Z., Liu, W., Zhang, X. & Zheng, F. 2009 Impacts of land use change and climate variability on hydrology in an agricultural catchment on the Loess Plateau of China. *Journal of Hydrology* **377** (1–2), 35–42. doi:10.1016/j.jhydrol.2009.08.007.

Li, D., Zhu, L., Xu, W. & Ye, C. 2022 Quantifying the impact of climate change and human activities on runoff at a tropical watershed in South China. *Frontiers in Environmental Science* **10**, 1023188. doi:10.3389/fenvs.2022.1023188.

Lin, K., He, Y. & Chen, X. 2012 Identifying the quantitative effect of climate change and human activity on runoff in the Dongjiang River basin. *Shuili Xuebao (Journal of Hydraulic Engineering)* **43** (11), 1312–1321. doi:10.13243/j.cnki.slxb.2012.11.001.

Lin, B., Chen, X., Yao, H., Chen, Y., Liu, M., Gao, L. & James, A. 2015 Analyses of landuse change impacts on catchment runoff using different time indicators based on SWAT model. *Ecological Indicators* **58**, 55–63. doi:10.1016/j.ecolind.2015.05.031.

Liu, Y., Ge, J., Guo, W., Cao, Y., Chen, C., Luo, X., Yang, L. & Wang, S. 2023 Revisiting biophysical impacts of greening on precipitation over the Loess Plateau of China using WRF with water vapor tracers. *Geophysical Research Letters* **50**, 8. doi:10.1029/2023GL102809.

Lou, S., Mo, L., Wang, Y. Q. & Zhou, J. Z. 2019 Trend analysis of monthly and annual runoff based on a segmented M-K method in Fuhe River basin, China. *IOP Conference Series: Earth and Environmental Science* **344**, 1. doi:10.1088/1755-1315/344/1/012108.

Ma, Z., Kang, S., Zhang, L., Tong, L. & Su, X. 2008 Analysis of impacts of climate variability and human activity on streamflow for a river basin in arid region of northwest China. *Journal of Hydrology* **352** (3–4), 239–249. doi:10.1016/J.JHYDROL.2007.12.022.

Miao, Z., Li, N., Lu, M. & Xu, L. 2021 Attribution analysis of runoff variations in the upper reaches of Hutuo River Basin. *Journal of Beijing Normal University (Natural Science)* **57** (06), 756–767. doi:10.12202/j.0476-0301.2020317.

Montanari, A., Young, G., Savenije, H. H. G., Hughes, D. A., Wagener, T., Ren, L., Koutsoyiannis,, D., Cudennec,, C., Toth,, E., Grimaldi,, S., Blöschl, G., Sivapalan, M., Beven, K. J., Gupta, H. V., Hipsey, M. R., Schaefli, B., Arheimer, B., Boegh, E., Schymanski, S. J., Baldassarre, G. D., Yu, B., Hubert, P., Huang, Y., Schumann, A. H., Post, D. A., Srinivasan, V., Harman, C., Thompson, S. E., Rogger, M., Viglione, A., McMillan, H. K., Characklis, G. W., Pang, Z. & Belyaev, V. R. 2013 'Panta Rhei–Everything Flows': Change in hydrology and society – The IAHS scientific decade 2013–2022. *Hydrological Sciences Journal* **58** (6), 1256–1275. doi:10.1080/02626667.2013.809088.

Ning, L., Xia, J., Zhan, C.-s. & Zhang, Y. 2016 Runoff of arid and semi-arid regions simulated and projected by CLM-DTVGM and its multi-scale fluctuations as revealed by EEMD analysis. *Journal of Arid Land* **8** (4), 506–520. doi:10.1007/s40333-016-0126-4.

Ren, C., Long, A., Yu, J., Yin, Z. & Zhang, J. 2021 Effects of climate and underlying surface changes on runoff of Yarkant River Source. *Arid Land Geography* **44** (05), 1373–1383. doi:10.12118/j.issn.1000 - 6060.2021.05.18.

Senbeta, T. B. & Romanowicz, R. J. 2021 The role of climate change and human interventions in affecting watershed runoff responses. *Hydrological Processes* **35**, 12. doi:10.1002/hyp.14448.

Sun, F., Yang, D., Liu, Z. & Cong, Z. 2007 Study on coupled water-energy balance in Yellow River basin based on Budyko hypothesis. *SHUILI XUEBAO* **38** (04), 409–416. doi:10.13243/j.cnki.slxb.2007.04.005.

Wang, L., Mu, X., Zhang, X. & Li, Y. 2008 Calculation method of mean rainfall amount of river basin in the hilly-gully region of Loess Plateau of Northern Shaanxi Province. *Science of Soil and Water Conservation* (02), 39–42. doi:10.16843/j.sswc.2008.02.007.

Wang, Y., Zhang, Q., Wang, J. & Zhang, L. 2017 Appling SWAT model to explore the impacts of land use and climate changes on the hydrological characteristics in Taohe River Basin. *Journal of Desert Research* **37** (01), 175–185. doi:10.7522/j.issn.1000-694X.2015.00189.

Wang, W., Lu, W., Xing, W., Li, J. & Li, C. 2018 Analysis of change and attribution of Budyko equation parameter n in Yellow River. *Water Resources Protection* **34** (02), 7–13. doi:10.3880/j.issn.1004-6933.2018.02.02.

Woo, B. S. & Shin, S. 2022 Rainfall trends analysis using Mann-Kendall and Spearman's rho tests: A case study of Gyeongsangbuk-do, Korea. *Crisis and Emergency Management: Theory and Praxis* **18** (6), 67–76. doi:10.14251/crisisonomy.2022.18.6.67.

Wu, J., Miao, C., Wang, Y., Duan, Q. & Zhang, X. 2017 Contribution analysis of the long-term changes in seasonal runoff on the Loess Plateau, China, using eight Budyko-based methods. *Journal of Hydrology* **545**, 263–275. doi:10.1016/J.JHYDROL.2016.12.050.

Wu, J., Zheng, H. & Xi, Y. 2019 SWAT-Based Runoff simulation and runoff responses to climate change in the headwaters of the Yellow River, China. *Atmosphere* **10**, 9. doi:10.3390/atmos10090509.

Xu, J. 2011 Variation in annual runoff of the Wudinghe River as influenced by climate change and human activity. *Quaternary International* **244** (2), 230–237. doi:10.1016/J.QUAINT.2010.09.014.

Xu, X., Yang, D., Yang, H. & Lei, H. 2014 Attribution analysis based on the Budyko hypothesis for detecting the dominant cause of runoff decline in Haihe basin. *Journal of Hydrology* **510**, 530–540. doi:10.1016/j.jhydrol.2013.12.052.

Xu, Z., Li, Y. P., Huang, G. H., Wang, S. & Liu, Y. R. 2021 A multi-scenario ensemble streamflow forecast method for Amu Darya River Basin under considering climate and land-use changes. *Journal of Hydrology* **598**. doi:10.1016/J.JHYDROL.2021.126276.

Xu, F., Zhao, L., Jia, Y., Niu, C., Liu, X. & Liu, H. 2022 Evaluation of water conservation function of Beijiang River basin in Nanling Mountains, China, based on WEP-L model. *Ecological Indicators* **134**. doi:10.1016/j.ecolind.2021.108383.

Xue, X. & Du, H. 2015 1:100,000 soil database in the upper reaches of the Yellow River (1995). *National Tibetan Plateau/Third Pole Environment Data Center*. More information available at: https://data.tpdc.ac.cn/zh-hans/data/30ccbda7-ead2-43e3-ada4-a9251b538c78/ [in Chinese, English information available].

Yang, H., Yang, D., Lei, Z. & Sun, F. 2008 New analytical derivation of the mean annual water-energy balance equation. *Water Resources Research* **44**, 3. doi:10.1029/2007wr006135.

Yang, D., Zhang, S. & Xu, X. 2015 Attribution analysis for runoff decline in Yellow River Basin during past fifty years based on Budyko hypothesis. *Science China: Technical Sciences* **45** (10), 1024–1034.

Yong, B., Ren, L., Hong, Y., Gourley, J. J., Chen, X., Dong, J., Wang, W., Shen, Y. & Hardy, J. 2013 Spatial–Temporal Changes of water resources in a typical semiarid basin of North China over the past 50 years and assessment of possible natural and socioeconomic causes. *Journal of Hydrometeorology* **14** (4), 1009–1034. doi:10.1175/JHM-D-12-0116.1.

Zhai, R. & Tao, F. 2017 Contributions of climate change and human activities to runoff change in seven typical catchments across China. *Science of the Total Environment* **605–606**, 219–229. doi:10.1016/j.scitotenv.2017.06.210.

Zhang, T., Zhu, X., Wang, Y., Li, H. & Liu, C. 2014 The impact of climate variability and human activity on runoff changes in the Huangshui River Basin. *Resources Science* **36** (11), 2256–2262.

Zhou, S., Yu, B., Huang, Y. & Wang, G. 2015 The complementary relationship and generation of the Budyko functions. *Geophysical Research Letters* **42** (6), 1781–1790. doi:10.1002/2015gl063511.

Zhou, S., Yu, B., Zhang, L., Huang, Y., Pan, M. & Wang, G. 2016 A new method to partition climate and catchment effect on the mean annual runoff based on the Budyko complementary relationship. *Water Resources Research* **52** (9), 7163–7177. doi:10.1002/2016wr019046.

Zhou, Z., Liu, J., Yan, Z., Wang, H. & Jia, Y. 2022 Attribution analysis of the natural runoff evolution in the Yellow River basin. *Advances in Water Science* **33** (01), 27–37. doi:10.14042/j.cnki.32.1309.2022.01.003.

First received 18 July 2023; accepted in revised form 11 February 2024. Available online 8 March 2024